

Chemical Science

Accepted Manuscript



This is an *Accepted Manuscript*, which has been through the Royal Society of Chemistry peer review process and has been accepted for publication.

Accepted Manuscripts are published online shortly after acceptance, before technical editing, formatting and proof reading. Using this free service, authors can make their results available to the community, in citable form, before we publish the edited article. We will replace this *Accepted Manuscript* with the edited and formatted *Advance Article* as soon as it is available.

You can find more information about *Accepted Manuscripts* in the [Information for Authors](#).

Please note that technical editing may introduce minor changes to the text and/or graphics, which may alter content. The journal's standard [Terms & Conditions](#) and the [Ethical guidelines](#) still apply. In no event shall the Royal Society of Chemistry be held responsible for any errors or omissions in this *Accepted Manuscript* or any consequences arising from the use of any information it contains.



www.rsc.org/chemicalscience

ARTICLE

Reversible CO₂ Binding Triggered by Metal-Ligand Cooperation in a Rhenium(I) PNP Pincer-Type Complex and the Reaction with Dihydrogen.

Cite this: DOI: 10.1039/x0xx00000x

Received 00th January 2012,
Accepted 00th January 2012

DOI: 10.1039/x0xx00000x

www.rsc.org/

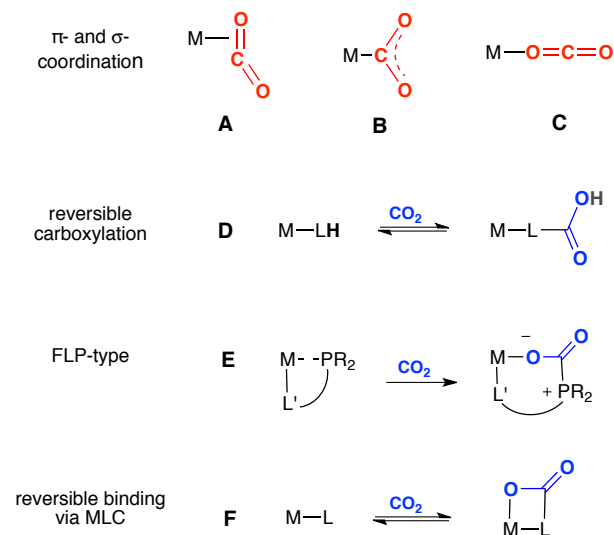
Matthias Vogt,^a Alexander Nerush,^a Yael Diskin-Posner,^b Yehoshoa Ben-David,^a and David Milstein^{a*}

ABSTRACT: Herein we report the reversible binding of CO₂ to a very rare dearomatized PNP pincer complex (*cis*-[Re(PNP^{tBu*})(CO)₂] **2**). The [1,3]-addition of CO₂ to the pincer complex is triggered by metal ligand cooperation via an aromatization/dearomatization sequence to form *cis*-[Re(PNP^{tBu-1}COO)(CO)₂] (**3**) via Re–O and C–C bond formation. The reversible binding was demonstrated by the exchange reaction of ¹³CO₂/CO₂ from the isotopically labelled compound *cis*-[Re(PNP^{tBu-13}COO)(CO)₂] (**3a**). Furthermore, complex **3** reacts with H₂ to give free CO₂ and the aromatized hydride complex [Re(PNP^{tBu})(CO)₂H] (**4**), which undergoes the reverse reaction to re-form **3** under CO₂ pressure at elevated temperature. Alternatively, **4** reacts, in a low temperature pathway, via the insertion of CO₂ into the Re–H bond to give the formate complex [Re(PNP^{tBu})(CO)₂(OOCH)] (**5**). Remarkably, complex **5** catalyses efficiently the dehydrogenation of formic acid under base-free conditions.

Introduction

The utilization of carbon dioxide as a C1 building block is a topic with growing importance in the chemical industry,^{1–3} and the catalytic transformation of this abundant gaseous feedstock into liquid fuels is an attractive goal with geopolitical and environmental implications.⁴ Naturally, catalytic conversion of CO₂, triggered by a homogeneous catalyst, requires initial binding of the CO₂ molecule to the catalyst prior to its chemical transformation. Commonly, the binding of CO₂ to a metal center proceeds via π -coordination of a C=O bond (Scheme 1, **A**) or formation of a σ -bond to the carbon atom (Scheme 1, **B**).⁵ Linear coordination of CO₂ through the oxygen atom is very rare,^{6,7} however its relevance in photosynthetic CO₂ fixation was proposed⁸ and it is discussed also in other biological systems.⁹ (Scheme 1, **C**). Alternative CO₂-binding modes, which include the participation of the ligand, have been recently reported. Song and co-workers describe a reversible carboxylation/decarboxylation of a diazaflourenide ligand in a Ru(II) complex at ambient temperature (Scheme 1, **D**).¹⁰ The binding of CO₂ to complexes, where the metal center and a pendant phosphine moiety function as a type of frustrated

Lewis acid / Lewis base pair (FLP, Scheme 1, **E**),¹¹ were reported by Wass and co-workers in zirconocene complexes with phosphinoaryloxy ligands.¹² Erker and co-workers described a FLP-reminiscent system based on a Zr⁺/P pair, which binds CO₂, forming Zr–O and P⁺–C bonds.¹³ Kemp and co-workers reported a homoleptic stannylyne compound with (P–P)-bis-chelating [(^tPr₂P)₂N)]₂ ligands, which are capable of binding two equivalents of CO₂.¹⁴ Dimeric zinc complexes with the (P–N)-bridging ligand [^tPr₂P–N(SiMe₃)] undergo multiple transformations when exposed to CO₂.¹⁵ FLP inspired binding of CO₂ to ruthenium tris(aminophosphine) complexes and phosphinoamide hafnium complexes have been reported by Stephan and co-workers.^{16,17} In a very recent report, Fontaine and co-workers describe the binding of CO₂ to tris(triphenylphosphine)aluminum via Al–O and P–C bond formation.¹⁸



Scheme 1. π - and σ -binding of CO_2 to a transition metal center (A-C) and binding of CO_2 to transition metal complexes under participation of the ligand (D-F).

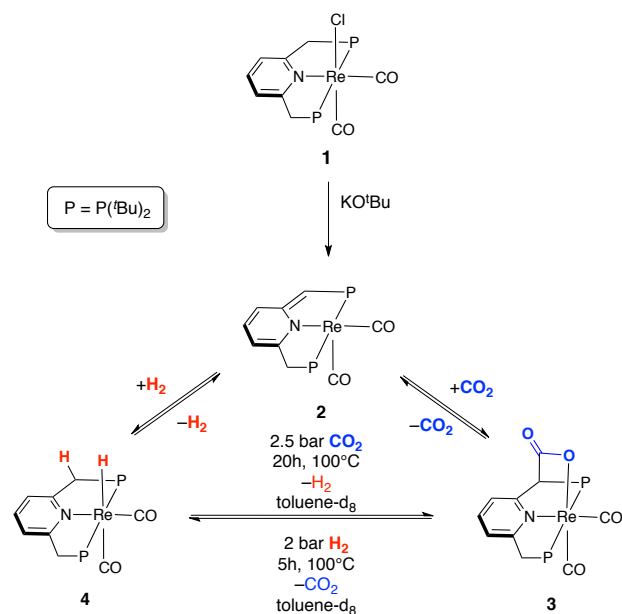
Bifunctional activation of CO_2 , in which nucleophilic carbon atoms take a key role, was published by Braunstein and co-workers in an early report on Pd(II) complexes with a $[\text{Ph}_2\text{P}-\text{CH}=\text{C}(\text{O})\text{OEt}]^-$ ligand¹⁹ and by Piers and co-workers in a scandium β -ketiminato complex.²⁰ We have recently reported a novel binding mode of CO_2 with reversible C–C and M–O bond formation triggered by metal-ligand cooperation (MLC) via an aromatization/dearomatization sequence in a Ru–PNP (PNP = 2,6-bis-(di-tert-butyl-phosphinomethyl)pyridine) pincer-type complex (Scheme 1, F).²¹ Both the ruthenium center and the *exo*-cyclic carbon of a dearomatized pincer ligand participate in the concerted [1,3]-addition of CO_2 to form the C–C and Ru–O bonds reversibly, with re-aromatization of the complex. Similar observations were made by Sanford and co-workers in a related Ru–PNN complex (PNN = (2-(di-tert-butylphosphinomethyl)-6-diethylaminomethyl)pyridine).²²

In recent years MLC took an important role in the development of efficient catalytic processes,^{23–32} including CO_2 reduction. Catalytic hydrogenation of CO_2 to formate salts was described by Nozaki and co-workers employing a highly active Ir(III)–PNP pincer complex,^{33,34} by Ikariya utilizing a well-defined system of a cooperative Ru(II) amide complex,³⁵ and by our group using a Fe(II)–PNP pincer complex under very mild reaction conditions.³⁶ Pidko and co-workers reported recently on the hydrogenation of CO_2 to formate salt catalysed by a Ru–PNP pincer complex, indicating that the cooperative CO_2 binding in that system has an inhibitory effect.³⁷ The hydrogenation of organic carbonates, carbamates, and formates using a dearomatized Ru(II) pincer complex as catalyst has been recently described by our group. This process opened a mild, low-pressure two-step hydrogenation pathway of CO_2 to methanol.³⁸ A catalytic cascade reaction to form methanol starting from CO_2 and H_2 using a combination of this complex with other catalyst has been reported by Sanford and co-workers.³⁹ With this background,⁴⁰ our group has focused on

the cooperative CO_2 -binding in transition metal pincer complexes.⁴¹ The reversible binding of CO_2 promoted by an aromatization/dearomatization sequence in the rhenium(I) complex $[\text{Re}(\text{PNP}^{\text{tBu}*})(\text{CO})_2]$ (**2**, the asterisk indicates the dearomatization of the ligand) and the reaction with H_2 will be discussed in this paper. Remarkably, reports on rhenium pincer complexes are very rare in the literature: Highly reactive amino-bisphosphino rhenium pincer polyhydrides have been previously reported by Caulton and co-workers,⁴² The heterolytic splitting of dihydrogen across a Re–N bond was described by Gusev and co-workers in an aliphatic pincer nitrosyl complex.⁴³ Recently, structurally well-defined Re nitrosyl complexes were reported by Berke and co-workers. These complexes are able to activate CO_2 via a cooperative mechanism employing a borane ($\text{B}(\text{C}_6\text{F}_5)_3$) and a Re–H moiety acting as FLP.⁴⁴ Aromatic, pyridine-based PNP rhenium pincer complexes are particularly rare. Walton and co-workers reported Re complexes decorated with PNP ligands, which gave rise to the formation of Re–Re multiple bonds.^{45,46} We have recently reported the Re–PNP pincer complex **2** as reactive species for the activation of $\text{C}\equiv\text{N}$ triple bonds of aromatic- and aliphatic nitriles triggered by MLC.⁴⁷

Results and Discussion

Complex **2** is readily prepared via deprotonation of the aromatic precursor *cis*- $[\text{Re}(\text{PNP}^{\text{tBu}})(\text{CO})_2\text{Cl}]$ (**1**).⁴⁷ Upon exposure of the deep green *n*-pentane solution of **2** to CO_2 (1 bar) a rapid discoloration is observed and the product *cis*- $[\text{Re}(\text{PNP}^{\text{tBu}}-\text{COO})(\text{CO})_2]$ (**3**) precipitates instantly as pale yellow solid in high yield (Scheme 2). The reaction proceeds via a [1,3]-addition of the CO_2 molecule to the *exo*-cyclic methine carbon of the pincer ‘arm’ and the Re metal center under C–C and Re–O bond formation. The NMR spectroscopic data is similar to that of the previously reported complex $[\text{Ru}(\text{PNP}^{\text{tBu}}-\text{COO})(\text{CO})\text{H}]$.²¹ The $^{31}\text{P}\{^1\text{H}\}$ NMR resonances of the AB system of **3** shifted to higher frequencies with respect to the starting complex **2** signifying the re-aromatization in **3**. Two doublets are observed in the spectrum (CD_2Cl_2 , 25°C) at 86.2 and 100.5 ppm with a coupling constant of $^2J_{\text{PP}} = 179.7$ Hz suggesting two phosphorus nuclei in different chemical environment. The characteristic resonance for the carboxylate carbon nucleus Re–OC(R)=O in the $^{13}\text{C}\{^1\text{H}\}$ NMR spectrum falls at 172.8 ppm and is observed as a doublet of doublets ($^2J_{\text{CP}} = 10.4$ Hz and $^4J_{\text{CP}} = 2.7$ Hz, C_6D_6 , 25°C). The IR vibrational spectrum has two strong absorptions at 1909 and 1828 cm^{-1} in a 1:1 ratio, consistent with two carbonyl ligands in mutual *cis* position. A third band characteristic of a carboxylate moiety is detected at 1647 cm^{-1} .



Scheme 2. Reversible reaction of complex 2 with CO₂ and H₂ to form complex 3 and 4, respectively.

Single crystals suitable for X-ray diffraction analysis were grown from a CH₂Cl₂ solution layered with *n*-pentane. The molecular structure of 3 (Figure 1) has an octahedral geometry. The PNP pincer ligand binds to the Re(I) center in a meridional fashion. The two CO ligands are in mutual *cis* position and the carboxylate ligand resides in an axial position. The newly formed C–C bond between the pincer arm and the carboxylate (C1–C24 = 1.565(5) Å) is elongated as compared, for example, to the C6–C7 single bond by 0.06 Å. This was similarly observed for the C1–C24 interatomic distance (1.562(2) Å) of [Ru(PNP^tBu–COO)(CO)H]. However, the Re1–O1 bond is significantly shorter than in the Ru1–O1 analog ($\Delta = 0.05$ Å) indicating a stronger binding of the CO₂ molecule in 3.

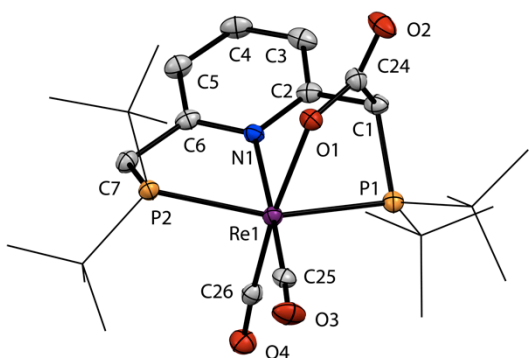
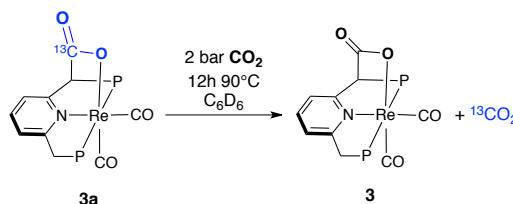


Figure 1. ORTEP drawing of [Re(PNP^tBu–COO)(CO)₂] (3) at 50 % ellipsoid probability (^tBu groups are drawn as wire frames). Hydrogen atoms and the co-crystallized CH₂Cl₂ solvent molecule are omitted for clarity. Selected bond lengths in Å: Re1–O1 = 2.202(3), Re1–N1 = 2.170(3); Re1–P1 = 2.424(1); Re1–P2 = 2.409(1); Re1–C25 = 1.898(4); Re1–C26 = 1.882(4), C1–C24 = 1.565(5), C24–O2 = 1.229(5), C24–O1 = 1.279(5), C25–O3 = 1.160(5), C26–O4 = 1.172(5), C1–C2 = 1.510(6), C6–C7 = 1.508(6).

The reversibility of the CO₂ binding via MLC is best demonstrated when the ¹³CO₂ labeled complex [Re(PNP^tBu–¹³COO)(CO)₂] (3a) is exposed to an atmosphere of non-labeled CO₂. Complex 3a in a C₆D₆ solution pressurized with 2 bar of CO₂ forms the non-labeled complex 3 within 12 h at 90 °C (Scheme 3). Figure 2 displays the region of the ¹³C{¹H} NMR spectrum correlated to the *exo*-cyclic carbon adjacent to the (¹³COO[–]) moiety (62.7 ppm). The spectrum of complex 3a has a doublet of doublets resonance with a large vicinal C–C coupling constant of ¹J_{CC} = 41.8 Hz and a smaller C–P coupling constant of ¹J_{CP} = 7.6 Hz (Figure 2, bottom). Upon formation of the non-labeled complex 3 the C–C coupling is not detected. (Figure 2, top).



Scheme 3. Exchange reaction of the bound ¹³CO₂ in complex 3a with non-labelled CO₂ to give complex 3.

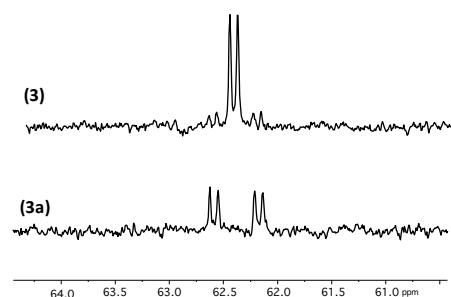
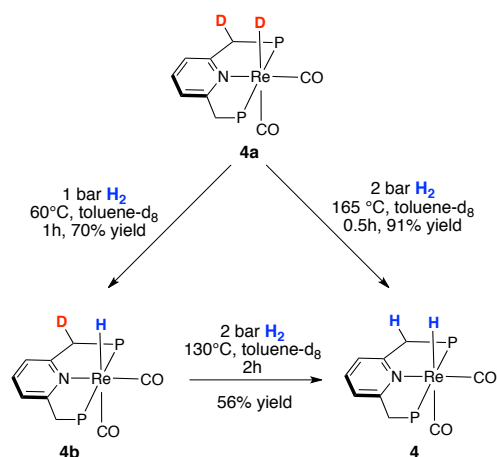


Figure 2. The region of the ¹³C{¹H} NMR spectrum (400.36 MHz, C₆D₆, 25 °C) of the benzylic CH(¹³COO) moiety of [Re(PNP^tBu–(¹³COO)(CO)₂]. Bottom: initial spectrum of the labeled complex 3a. Top: Resulting spectrum of the non-labelled complex 3 after 12 h at 90 °C under 2 bar CO₂ pressure.

Reaction of 3 with dihydrogen: The reaction of a toluene-d₈ solution of complex 3 with dihydrogen gas (2 bar) results in formation of the hydride complex *cis*-[Re(PNP^tBu)(CO)₂H] (4) and free CO₂ (Scheme 2). This reaction is slow at room temperature. Only traces of 4 can be detected by ¹H and ³¹P{¹H} NMR spectroscopy after 20 h. The exchange is significantly faster at elevated temperature. Heating the sample for five hours at 100 °C resulted in quantitative displacement of CO₂ from 3 and exclusive formation of 4. We have previously reported the activation of H₂ triggered by MLC in dearomatized pyridine-based PNP pincer complexes of various transition metals.^{48–51} The dearomatized complex 2 is also capable of splitting dihydrogen heterolytically via the Re metal center and the *exo*-cyclic methine carbon of the pincer arm under Re–H and C–H bond formation. The hydride complex 4 was independently obtained from the reaction of complex 2 in *n*-pentane solution and H₂ gas. The ³¹P{¹H} NMR spectrum of 4 has a singlet centered at 80.8 ppm indicating two phosphorus nuclei in an identical chemical environment. The ¹H NMR spectrum (C₆D₆,

25°C) has a characteristic hydridic resonance at -2.29 ppm observed as virtual triplet ($^2J_{\text{HP}} = 22.42$ Hz) as a result of the coupling to two chemically identical phosphorus nuclei with similar $^2J_{\text{HP}}$ coupling constants. Two proton resonances of the pyridine moiety fall in the aromatic regime signaling the re-aromatization in complex **4**: A virtual triplet is observed at 6.73 ppm ($^3J_{\text{HH}} = 7.61$ Hz), which correlates with the *para*-CH proton of the pyridine ring. A doublet at 6.41 ppm ($^3J_{\text{HH}} = 7.61$ Hz), integrating to two protons, relates to both chemically identical *meta*-CH protons. The benzylic methylene protons of the pincer arms give rise to two doublets of (virtual) triplets resonances at 3.12 and 3.19 ppm as a result of a large geminal coupling ($^2J_{\text{HH}} = 16.00$ Hz), a vicinal H-H coupling to the ^1H nucleus of the Re-H moiety, and H-P coupling with similar $^3J_{\text{HP}}$ coupling constant. The IR spectrum shows two strong bands at 1890 and 1848 cm^{-1} in approximately 1:1 ratio indicating a mutual *cis*-position of both CO ligands. The Re-H moiety gives rise to a strong absorbance at 1778 cm^{-1} . The reaction of **2** with D_2 under the same conditions yielded the Re deuteride complex ($[\text{Re}(\text{PNP}^{\text{tBu}}\text{-D})(\text{CO})_2\text{D}]$, **4a**). Formation of the Re-D moiety occurs concomitantly with the incorporation of exclusively one deuterium atom into the *exo*-cyclic CH_2 moiety (for NMR spectra see *Electronic Supplementary Information (ESI)*, Figure S12–S16). At room temperature, under D_2 gas, H/D scrambling was not observed for the protons of the CH_2 moieties. This selective reaction suggests that the heterolytic D_2 splitting occurs intramolecularly between the Re center and the methine carbon of the pincer arm on the same face of the pincer ligand.⁵²



Scheme 4. Reaction of the deuterium labelled complex **4a** with H_2 gas.

A drastic color change from yellow to deep green, characteristically of the dearomatized species **2**, is observed when a toluene solution of complex **4** is heated to 175°C in a sealed NMR tube (Scheme 2), suggesting dihydrogen liberation from **4** via the reverse of MLC hydrogen splitting reaction. To further investigate the reversibility of the H_2 binding in complex **4a**, a solution of the complex in toluene-d_8 , was pressurized with 1 bar of H_2 gas and the reaction was followed by ^1H NMR spectroscopy at variable temperatures (for NMR spectra see *ESI*, Figure S18–S21). Initially the H/D exchange was exclusively observed for the Re-D moiety at temperatures $< 65^\circ\text{C}$ (70% yield of **4b** after 1 h at 60°C). The deuterium in the pincer arm remains present. This observation may

suggest a hydride/deuteride exchange reaction with no participation of a MLC process at the indicated temperature.⁵³ Increasing the H_2 pressure to 2 bars and heating the sample at 130°C for 2 h gave a quantitative H/D exchange for the Re-D moiety and 56% H/D exchange was observed for the benzylic *CHD* moiety of the pincer arm.⁵⁴ When the sample was heated for 0.5 h at 160°C and a hydrogen pressure of 2 bars was applied, nearly complete (91%) H/D exchange occurred and complex **4** was re-formed, (Scheme 4).

Reaction of **4 with CO_2 :** Remarkably, complex **4** in toluene-d_8 under CO_2 pressure (2.5 bar) reacts back to the [1,3]-addition product **3** (Scheme 2). Upon heating at 100°C for 20 h complex **4** is transformed to **3** and free H_2 gas in 75% conversion. In contrast, the reaction at lower temperature gives the rhenium formate complex *cis*- $[\text{Re}(\text{PNP}^{\text{tBu}})(\text{CO})_2(\text{OOCH})]$ (**5**) as a result of the insertion of CO_2 into the metal-hydride bond, (Scheme 5). The reaction is slow at room temperature, only minor formation of **5** being observed after 24 h. The insertion can be accelerated by heating to 50°C . After 70 h complex **5** is obtained in 77% yield. The reaction can be followed by NMR spectroscopy. Representative ^1H NMR spectra at variable temperatures are displayed in Figure 3. The rhenium formate complex formation is reversible. Complex **5** is transformed back to the hydride species **4** at temperatures above 75°C (Figure 3, top spectrum, 1 h at 363 K).

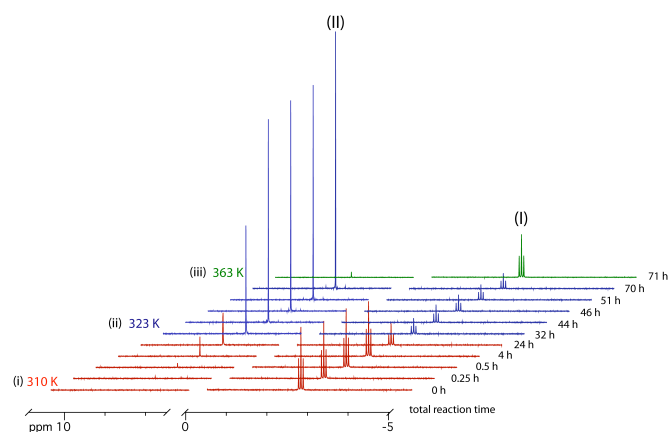
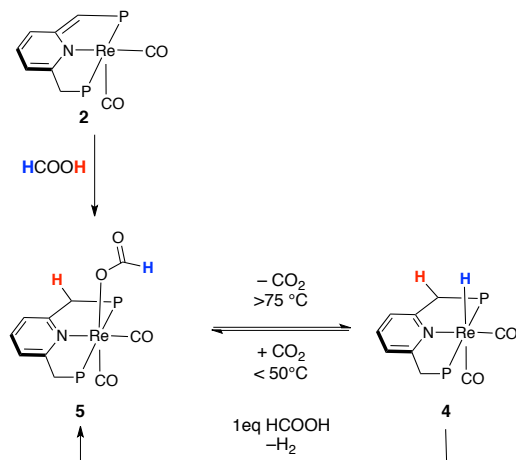


Figure 3. Section of the ^1H NMR spectra of the reaction of **4** in C_6D_6 with CO_2 (2 bar, i) 310 K red; ii) 323 K blue; iii) 363 K green). (I): hydridic resonance of **4** (t, -2.29 ppm, $^2J_{\text{HP}} = 22.42$ Hz). (II): Formate Re-OOCH resonance (s, 8.94 ppm).

Complex **5** was independently obtained by the reaction of **2** with formic acid in *n*-pentane. Upon addition of the acid a pale yellow product precipitates instantaneously from the solution. The $^{31}\text{P}\{^1\text{H}\}$ NMR spectrum (C_6D_6 , 25°C) of the obtained complex **5** exhibits a singlet resonance at 72.3 ppm for two chemically identical phosphorus nuclei. The resonance is shifted to higher frequencies with respect to **2**, indicating the re-aromatization of **5**. The ^1H NMR spectrum exhibits a characteristic singlet for the coordinated formate moiety Re-OOCH at 8.94 ppm and, consistently, the $^{13}\text{C}\{^1\text{H}\}$ NMR spectrum shows the correlated resonance for the Re-OOCH moiety at 170.8 ppm. The IR spectrum exhibits two strong absorbances for the carbonyl ligands at 1907 and 1824 cm^{-1} in a 1:1 ratio indicating a mutual *cis*-position and a OC-Re-CO angle of 90° . A strong absorbance associated with the formate ligand appears at 1630 cm^{-1} .

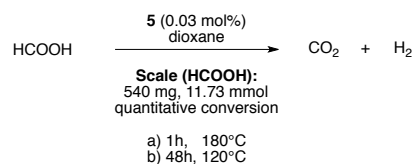
Complex **5** can be alternatively obtained by protonation of the hydride in complex **4** with formic acid (Scheme 5). Upon addition of HCOOH to complex **4** in a toluene- d_8 solution a rapid color change from yellow to pale yellow is observed, accompanied by vigorous formation of gas bubbles in the solution.



Scheme 5. Synthesis pathways for complex **5** and CO₂ elimination to form **4**.

Catalytic dehydrogenation of formic acid. Formic acid is envisioned as a hydrogen storage/carrier material, for instance for the operation of fuel cells. Highly efficient dehydrogenation catalysts have been developed. Base-free reaction conditions are desirable because the (sub)-stoichiometric use of base lowers the hydrogen storage capacity.⁵⁵⁻⁵⁸ Our stoichiometric studies showed that the formate complex **5** liberates CO₂ at elevated temperatures (>75 °C) forming the hydride complex **4**. Reformation of **5** occurs via the reaction of **4** and formic acid, with hydrogen liberation, which outlines a catalytic pathway (Scheme 5). We have recently reported that the iron-based PNP pincer complex [Fe(PNP^{tBu})(CO)H] catalyzes efficiently hydrogen liberation from formic acid.⁵⁹ In this process metal-hydride and formate species play important roles as intermediates in the dehydrogenation reaction. When complex **5** (0.03 mol%) and formic acid (11.7 mmol scale) were heated in dioxane, in a closed system at 120 °C, formation of CO₂ and H₂ was observed. However, extended reaction times are required (82% yield after 24 h; >99% yield after 48 h). Remarkably, there is no need for added base.⁶⁰ A more efficient dehydrogenation occurs at higher temperatures. When the reaction is carried out at 175–180 °C (oil bath temperature) in a Fischer-Porter tube, formic acid is rapidly and quantitatively transformed into CO₂ and H₂ (Scheme 6 and Experimental Section for details).⁶¹

Although the reaction is driven under rather harsh conditions, CO is not formed in the course of the reaction. Small catalyst loadings (0.03 mol%) are very effective. After the catalytic reaction was completed (verified by ¹H NMR spectroscopy, full conversion of HCOOH) all volatiles were removed from the mixture *in vacuo*. The yellow residue contained complexes **4** and **5** as the major compounds, demonstrating a remarkable stability of the rhenium pincer complexes under the applied reaction conditions.



Scheme 6. Dehydrogenation of formic acid catalysed by complex **5**.

Summary and Conclusion

In summary, we have described the reversible binding of CO₂ to the dearomatized rhenium complex [Re(PNP^{tBu*})(CO)₂] (**2**) triggered by MLC. The binding of CO₂ involves reversible C–C and Re–O bond formation with an aromatization/dearomatization sequence of the PNP ligand to give *cis*-[Re(PNP^{tBu}-COO)(CO)₂] (**3**). In contrast to our previously reported ruthenium complex [Ru(PNP^{tBu}-COO)(CO)H], which releases CO₂ readily at room temperature, the CO₂ in **3** is bound more strongly. This is reflected in the elevated temperature (90 °C) required for the exchange reaction **3a** + CO₂ → **3** + ¹³CO₂. Complex **3** reacts with dihydrogen with release of CO₂ and formation of the aromatized hydride complex *cis*-[Re(PNP^{tBu})(CO)₂H] (**4**). Complex **4**, on the other hand, can react with CO₂ in two different pathways: Firstly, the low-temperature (< 50 °C) “classical” pathway entails the insertion of CO₂ into the Re–H bond to give the formate complex [Re(PNP^{tBu})(CO)₂(OOCH)] (**5**). Secondly, the cooperative high-temperature pathway (> 75 °C) leads to the displacement of dihydrogen from **4** and re-formation of **3**. A temperature dependent dual reactivity is similarly observed, when the deuterium labeled complex [Re(PNP^{tBu}-D)(CO)₂(D)] (**4a**) was reacted with H₂ gas. At lower temperatures H/D exchange was only detected for the Re–D moiety. Complete H/D exchange, including the deuterium incorporated in the pincer arm, was observed only at higher temperatures. Complex **5** was employed as efficient catalyst for the base-free dehydrogenation of formic acid. The hydrogen liberation proceeds rapidly and selectively above 175 °C suggesting that MLC is involved in the liberation process.

Experimental Section

All experiments were performed under an atmosphere of purified nitrogen in a M-BRAUN Unilab 1200/780 glovebox or using standard Schlenk techniques. All solvents were purchased “reagent grade” or better. Solvents, except methylene chloride, were refluxed over sodium/benzophenone and distilled under an argon atmosphere. Methylene chloride was used as received and dried over 4 Å molecular sieves. Deuterated solvents were used as received and degassed with argon and kept in the glovebox over 4 Å molecular sieves. Complexes [Re(PNP^{tBu})(CO)₂Cl] (**1**) and [Re(PNP^{tBu*})(CO)₂] (**2**) were prepared according to the literature procedure.⁴⁷ KOTBu (Sigma-Aldrich), CO₂ (Linde, 99.998%), Hydrogen (Gordon Gas and Chemicals Ltd, 99.999%), ¹³CO₂ and D₂ (Cambridge Isotope Labs) was used as received without further purification. **NMR Spectroscopy:** ¹H-, ¹³C{¹H}- and ³¹P{¹H} NMR spectra were recorded on Bruker AMX-300, AMX-400, and AMX-500 NMR spectrometers. ¹H-, ¹³C{¹H}-, and ¹³C{¹H}-DEPTQ NMR

chemical shifts are reported in ppm referenced to tetramethylsilane. $^{31}\text{P}\{^1\text{H}\}$ NMR chemical shifts are reported in ppm referenced to an external 85% solution of phosphoric acid in D_2O . **Elemental Analyses** was performed on a Thermo Finnigan Italia S.p.A-FlashEA 1112 CHN Elemental Analyzer by the Department of Chemical Research Support, Weizmann Institute of Science. **Mass spectra** were recorded on MicromassPlatform LCZ 4000, using Electro Spray Ionization (ESI) mode. **IR spectra** were recorded on a Nicolet FT-IR spectrometer. **GC- Analysis** were performed on a GOW-MAC Instruments, Series 400 G/C gas chromatograph with thermal conductivity detector (TCD) with Carbonplot capillary (J&W Scientific) and on a Hewlett Packard HP 6890 series with TCD equipped with a ShinCarbon ST 80/100 Micropack column (2m x 0.53mm). Helium was used as carrier gas. **Crystallographic Details:** *Crystal Data:* $\text{C}_{26}\text{H}_{42}\text{NO}_4\text{P}_2\text{Re} + \text{CH}_2\text{Cl}_2$, light yellow prism 0.10 x 0.05 x 0.05 mm³, Monoclinic $P2_1/c$, $a = 13.2321(1) \text{ \AA}$, $b = 15.7048(3) \text{ \AA}$, $c = 16.7382(2) \text{ \AA}$, $\beta = 114.8330(5)^\circ$, from 30° of data and 9124 reflections, $T = 120(2)\text{K}$, $V = 3156.70(5)\text{\AA}^3$, $Z = 4$, $F_w = 765.67$, $D_c = 1.611 \text{ Mg m}^{-3}$, $\mu = 4.152 \text{ mm}^{-1}$. Data was collected on a Nonius Kappa CCD diffractometer (MoK α , $\lambda = 0.71073\text{\AA}$) with graphite monochromator. $-18 \leq h \leq 16$, $0 \leq k \leq 21$, $0 \leq l \leq 23$, 69065 reflections collected, 9189 independent reflections ($R_{\text{int}} = 0.057$). The data were processed with DENZO-HKL-Scalepack. The structure was solved with SIR-97. Full matrix least-squares refinement based on F^2 with SHELXL-97 on 347 parameters with no restraints gave final $R_1 = 0.0384$ (based on F^2) for data with $I > 2\sigma(I)$ and $R_1 = 0.0529$ on 8863 reflections, goodness-of-fit on $F^2 = 1.109$. CCDC 973497 (for complex **3**) contains the supplementary crystallographic information file and can be obtained free of charge from The Cambridge Crystallographic Data Centre via www.ccdc.cam.ac.uk/data_request/cif.

Catalytic dehydrogenation of formic acid: A Fischer-Porter tube (95 mL total volume), equipped with a magnetic stirring bar, was charged with **5** (2.5 mg, 0.0037 mmol, 0.03 mol% with respect to HCOOH) dissolved in 2 mL dioxane and subsequently formic acid (540 mg, 11.731 mmol) was added to form a pale yellow solution. *Experiment at 180°C:* A Fischer-Porter tube containing the reaction mixture was heated to 180 °C (oil bath temperature). After 1 h a pressure of 9 bar was detected in the tube. Completion of the reaction was indicated by a color change of the mixture to deep yellow. The tube was cooled to ambient temperature and subsequently to 0 °C in an ice/water bath. After 10 min, the pressure in the tube equilibrated at 5.5 bar, which correlates to a obtained gas volume of 522.5 mL (23.007 mmol) at 1 bar using the ideal gas law as approximation (theoretically, 100% conversion $\text{HCOOH} \rightarrow \text{CO}_2 + \text{H}_2 = 23.463 \text{ mmol}$, 532.9 mL gas at 1 bar). *Analysis of the formed gas mixture:* An IR cell, designed for gaseous sample analysis, was purged with the formed gas mixture directly from the Fischer-Porter tube. The obtained IR spectrum showed a strong absorbance for CO_2 . Absorbance correlated to carbon monoxide was not detected. GC analysis of the gas confirmed H_2 and CO_2 as reaction products in a 1:1 ratio. *Analysis of non-gaseous components:* After release of the pressure from the tube, a sample of the reaction mixture was taken and diluted in CDCl_3 . No residual formic acid was detected in the performed NMR spectroscopic

analysis (full conversion of HCOOH). Subsequently, all volatiles were removed *in vacuo* and the yellow residue was dissolved in C_6D_6 and analyzed by NMR spectroscopy. The $^{31}\text{P}\{^1\text{H}\}$ and ^1H NMR spectra exhibit the characteristic resonances of complex **5** and **4** as major components. *Experiment at 120°C:* A Fischer-Porter tube (95 mL total volume) containing the reaction mixture was heated to 120 °C (oil bath temperature). After 24 h a pressure of 5.5 bar was detected in the tube. The tube was cooled to ambient temperature and subsequently to 0 °C in an ice/water bath. After 10 min, the pressure in the tube equilibrated at 4.6 bar, which correlates to 436 mL total gas volume at 1 bar and a conversion of 82%. Full conversion was achieved after 48 h (no residual formic acid was detected in the ^1H NMR spectroscopic analysis, full conversion of HCOOH). *Experiment under reflux in open system:* A Schlenk tube equipped with a stirring bar and a reflux condenser, was charged with **5** (2.5 mg, 0.0037 mmol, 0.03 mol% with respect to HCOOH) dissolved in 2 mL dioxane. Subsequently, formic acid (540 mg, 11.731 mmol) was added to form a pale yellow solution. The mixture was heated under reflux and the formed gases were collected in a graduated cylinder, which was filled with silicon oil, inverted, and placed in a pneumatic trough containing silicon oil, as well. The exit of the outlet tube (connected to the top of the reflux condenser on the other side) was inserted into the opening of the cylinder. The formed gas bubbled up and displaced the silicon oil in the cylinder. After 24h of reaction time a volume of 155 mL (27% yield), and after 48 h 255 mL (44% yield) was collected. *Control Experiment:* A Fischer-Porter tube (95 mL total volume), equipped with a magnetic stirring bar, was charged with formic acid ((540 mg, 11.731 mmol) in 2 mL of dioxane. The tube was heated to 180 °C (oil bath temperature). After 1 h no over-pressure was detected in the tube.

cis-[Re(PNP^{tBu}-COO)(CO)₂] (3**):** KOtBu (17 mg, 0.15 mmol, 1 equiv.) was added to a stirred solution of **1** (100 mg, 0.15 mmol) in 4 mL THF in a 20 mL vial. After 10 min all volatiles were evaporated *in vacuo* and the residue was extracted with *n*-pentane (20 mL). The obtained deep green extract solution was filtered through a syringe filter (Teflon, 0.2 μm pore size). Subsequently, CO_2 gas was bubbled through the solution (ca. 25 mL via syringe) and an immediate color change to yellow occurred followed by the precipitation of a yellow powder. The vial was kept at -36 °C for 12 h to finish the precipitation. The product was decanted from the almost colorless supernatant solution, washed with *n*-pentane (5 mL) and dried *in vacuo*. Yield: 90 mg, 88 %. ^1H NMR (400.36 MHz, C_6D_6 , 25°C) δ : 0.80 (d, $^3J_{\text{PH}} = 12.41 \text{ Hz}$, 9H, (CH₃)₃CP), 0.96 (d, $^3J_{\text{PH}} = 12.41 \text{ Hz}$, 9H, (CH₃)₃CP), 1.39 (d, $^3J_{\text{PH}} = 13.21 \text{ Hz}$, 9H, (CH₃)₃CP), 1.56 (d, $^3J_{\text{PH}} = 13.21 \text{ Hz}$, 9H, (CH₃)₃CP), 3.03 (dd, $^2J_{\text{HH}} = 16.01 \text{ Hz}$, $^2J_{\text{HP}} = 5.20 \text{ Hz}$, 1H, PCH₂), 3.32 (dd, $^2J_{\text{HH}} = 16.01 \text{ Hz}$, $^2J_{\text{HP}} = 9.61 \text{ Hz}$, 1H, PCH₂), 4.88 (dd, $^2J_{\text{HP}} = 6.00 \text{ Hz}$, $^4J_{\text{HP}} = 2.00 \text{ Hz}$, 1H PCH), 6.45 (d, $^3J_{\text{HH}} = 7.61 \text{ Hz}$, 1H, CH_{py}), 6.77 (d, $^3J_{\text{HH}} = 7.61 \text{ Hz}$, 1H, CH_{py}), 6.87 (t, $^3J_{\text{HH}} = 7.61 \text{ Hz}$, 1H, CH_{py(4)}) ppm. $^{31}\text{P}\{^1\text{H}\}$ NMR (162.1 MHz, CD_2Cl_2 , 25°C) δ : 86.2 (d, $^2J_{\text{PP}} = 179.7 \text{ Hz}$, 1P), 100.5 (d, $^2J_{\text{PP}} = 179.7 \text{ Hz}$, 1P) ppm. $^{13}\text{C}\{^1\text{H}\}$ QDEPT NMR (100.7 MHz, C_6D_6 , 25°C) δ : 29.3 (d, br, $^2J_{\text{CP}} = 3.8 \text{ Hz}$, 3C, (CH₃)₃CP), 29.8 (d, br, $^2J_{\text{CP}} = 2.8 \text{ Hz}$, 3C, (CH₃)₃CP), 30.3 (d, $^2J_{\text{CP}} = 4.5 \text{ Hz}$, 3C, (CH₃)₃CP), 30.4 (d, $^2J_{\text{CP}} = 3.8 \text{ Hz}$, 3C,

(CH₃)₃CP), 37.3 (dd, ¹J_{CP} = 9.7 Hz, ³J_{CP} = 4.6 Hz, 1C, (CH₃)₃CP), 37.8 (m, overlay, 2C, (CH₃)₃CP), 38.5 (d, ¹J_{CP} = 21.3 Hz, 1C, (CH₃)₃CP), 39.5 (d, ¹J_{CP} = 18.0 Hz, 1C, PCH₂), 61.9 (d, ¹J_{CP} = 7.6 Hz, 1C, PCH-COO), 119.8 (d, ³J_{PC} = 5.6 Hz, 1C, CH_{py}), 120.1 (d, ³J_{PC} = 6.7 Hz, 1C, CH_{py}), 138.9 (s, 1C, CH_{py(4)}), 161.0 (t, J_{PC} = 3.8 Hz, 1C, C_{py}), 164.1 (br, m, 1C, C_{py}), 172.8 (dd, ²J_{CP} = 10.4 Hz, ⁴J_{CP} = 2.7 Hz, 1C, Re-O-C=O), 207.7 (br, t, ²J_{CP} = 5.0 Hz, 1C, Re-CO), 209.3 (br, dd, ²J_{CP} = 6.0 Hz, ²J_{CP} = 5.3 Hz, 1C, Re-CO) ppm. IR (KBr, pellet) ν[cm⁻¹]: 1909, 1828 (ν_{CO}, 1:1 ratio), 1647 (ν_{CO}). Elemental analysis: (C₂₆H₄₂N₁O₄P₂Re) calculated (found): C 45.87 (45.94) H 6.22 (6.12) N 2.06 (1.91) %. MS (ESI-TOF) calc. 681.21; found M⁺ = 704.22 (3 + Na⁺), 638.04 (3 - CO₂ + H⁺).

CO₂ / H₂ exchange in cis-[Re(PNP^{tBu}-COO)(CO)₂] (3): A *J. Young* NMR tube, fitted with a *Kontes* valve, was charged with complex **3** (10 mg, 0.015 mmol), dissolved in 0.5 mL toluene-d₈ and pressurized with 2 bar H₂. The exchange reaction was monitored by ¹H and ³¹P{¹H} NMR spectroscopy. After 20 h at ambient temperature complex **4** was formed in ca. 5 % yield. Heating the tube for 5 h at 100°C gave complex **4** in 100% yield.

cis-[Re(PNP^{tBu}-¹³COO)(CO)₂] (3a): A NMR tube fitted with rubber septum was charged with complex **2** (10 mg, 0.016 mmol), dissolved in 0.6 mL C₆D₆. Subsequently, ¹³CO₂ gas (ca. 2 mL) was injected via syringe into the NMR tube. The green solution turned instantly yellow, indicating completion of the reaction. The solution was degassed (no resonance for free ¹³CO₂ gas was observed in the ¹³C{¹H} NMR spectrum) to give compound **3a** in quantitative yield. ¹H NMR (400.36 MHz, C₆D₆, 25°C) δ: 0.80 (d, ³J_{PH} = 12.41 Hz, 9H, (CH₃)₃CP), 0.93 (d, ³J_{PH} = 12.41 Hz, 9H, (CH₃)₃CP), 1.37 (d, ³J_{PH} = 13.21 Hz, 9H, (CH₃)₃CP), 1.56 (d, ³J_{PH} = 13.21 Hz, 9H, (CH₃)₃CP), 2.97 (dd, ²J_{HH} = 16.01 Hz, ²J_{HP} = 5.20 Hz, 1H, PCH₂), 3.25 (dd, ²J_{HH} = 16.01 Hz, ²J_{HP} = 9.61 Hz, 1H, PCH₂), 4.89 (m, ddd overlay, ²J_{HP} ~ 6.0 Hz, ²J_{HC} = ⁴J_{HP} ~ 2.0 Hz, 1H PCH), 6.39 (d, ³J_{HH} = 8.00 Hz, 1H, CH_{py}), 6.75 (d, ³J_{HH} = 7.60 Hz, 1H, CH_{py}), 6.85 (t, ³J_{HH} = 7.61 Hz, 1H, CH_{py(4)}) ppm. ³¹P{¹H} NMR (125.1 MHz, C₆D₆, 25°C) δ: 84.5 (d, ²J_{PP} = 182.0 Hz, 1P), 98.6 (dd, ²J_{PP} = 182.0 Hz, ²J_{PC} = 9.9 Hz, 1P) ppm. ¹³C{¹H} QDEPT NMR (100.7 MHz, C₆D₆, 25°C) δ: 29.7 (d, ²J_{CP} = 3.8 Hz, 3C, (CH₃)₃CP), 29.9 (d, ²J_{CP} = 3.1 Hz, 3C, (CH₃)₃CP), 30.6 (d, ²J_{CP} = 3.6 Hz, 3C, (CH₃)₃CP), 30.7 (d, ²J_{CP} = 4.1 Hz, 3C, (CH₃)₃CP), 37.4 – 37.9 (m, overlay, 3C, (CH₃)₃CP), 38.3 (d, ¹J_{CP} = 21.0 Hz, 1C, (CH₃)₃CP), 39.5 (d, ¹J_{CP} = 17.1 Hz, 1C, PCH₂), 62.7 (dd, ¹J_{CC} = 41.8 Hz, ¹J_{CP} = 7.6 Hz, 1C, PCH-COO), 119.3 (d, ³J_{PC} = 6.5 Hz, 1C, CH_{py}), 119.5 (d, ³J_{PC} = 5.6 Hz, 1C, CH_{py}), 137.9 (s, 1C, CH_{py(4)}), 163.0 (br, m, 1C, C_{py}), 164.1 (br, m, 1C, C_{py}), 172.8 (dd, intense signal, ²J_{CP} = 10.4 Hz, ⁴J_{CP} = 2.4 Hz, 1C, Re-O-C=O), 208.1 (br, s, 1C, Re-CO), 209.4 (br, s, 1C, Re-CO) ppm. **¹³CO₂ / CO₂ exchange in cis-[Re(PNP^{tBu}-¹³COO)(CO)₂] (3a), Figure 2:** The obtained solution (see above) of **3a** (0.016 mmol in 0.6 mL C₆D₆) was transferred into a *J. Young* NMR tube, fitted with a *Kontes* valve, and pressurized with 2 bar CO₂. The exchange reaction was monitored via ¹³C{¹H} NMR spectroscopy. Heating at 90°C for 12 h gave **3**.

cis-[Re(PNP^{tBu})(CO)₂H] (4): KO^tBu (10 mg, 0.09 mmol, 1 equiv.) was added to a stirred solution of **1** (60 mg, 0.09 mmol) in 3 mL THF in a 20 mL vial. After 10 min all volatiles were evaporated *in vacuo* and the residue extracted in *n*-pentane (15 mL)

and filtered through a syringe filter (Teflon, 0.2 μm pore size). Subsequently, H₂ gas was bubbled through the solution via cannula and an immediate color change to intense yellow occurred. Small yellow micro crystals were formed upon cooling to -36 °C. After 12 h the crystals were decanted from the supernatant solution, washed with cold *n*-pentane and dried *in vacuo*. The recovered mother liquor was kept in a 20 mL vial at -36 °C for additional 12 h. To finish the precipitation, the mother liquor was concentrated to ca. 2 mL and treated alike to give a second fraction of yellow micro crystals of **4**. Yield: 47 mg, 82 %. ¹H NMR (400.36 MHz, C₆D₆, 25°C) δ: -2.29 (vt, ²J_{HP} = 22.42 Hz, 1H, Re-H), 1.28 (vt, AA'BB', ³J_{PH} = 6.40 Hz, 18H, (CH₃)₃CP), 1.37 (vt, AA'BB', ³J_{PH} = 6.40 Hz, 18H, (CH₃)₃CP), 3.12 (dt, ²J_{HH} = 16.00 Hz, J = 2.50 Hz, 2H, PCH₂), 3.19 (dt, ²J_{HH} = 16.00 Hz, J = 3.55 Hz, 2H, PCH₂), 6.41 (d, ³J_{HH} = 7.61 Hz, 2H, CH_{py}), 6.73 (t, ³J_{HH} = 7.61 Hz, 1H, CH_{py(4)}), ppm. ³¹P{¹H} NMR (162.1 MHz, C₆D₆, 25°C) δ: 80.8 (s, 2P) ppm. ¹³C{¹H} NMR (100.7 MHz, C₆D₆, 25°C) δ: 29.6 (vt, ²J_{CP} = 2.2 Hz, 6C, (CH₃)₃CP), 29.7 (vt, ²J_{CP} = 2.5 Hz, 6C, (CH₃)₃CP), 35.2 (t, ¹J_{CP} = 10.3 Hz, 2C, (CH₃)₃CP), 37.3 (d, ¹J_{CP} = 8.0 Hz, 2C, (CH₃)₃CP), 41.8 (t, ¹J_{CP} = 7.6 Hz, 2C, PCH₂), 118.6 (br, t, ³J_{PC} = 3.9 Hz, 2C, CH_{py}), 134.1 (s, 1C, CH_{py(4)}), 164.7 (t, J_{PC} = 4.6 Hz, 2C, C_{py}), 208.5 (t, ²J_{CP} = 5.2 Hz, 1C, Re-CO), 208.6 (t, ²J_{CP} = 5.5 Hz, 1C, Re-CO) ppm. IR (KBr, pellet) ν[cm⁻¹]: 1890, 1848 (ν_{CO}, approximately 1:1 ratio), 1778 (ν_{Re-H}). Elemental analysis: (C₂₅H₄₄N₁O₂P₂Re) calculated (found): C 47.01 (47.17) H 6.94 (7.00) N 2.19 (1.78) %. MS (ESI-TOF) calc. 639.24; found M⁺ = 638.36 (4⁺).

H₂ / CO₂ exchange in cis-[Re(PNP^{tBu})(CO)₂H] (4): A *J. Young* NMR tube fitted with a *Kontes* valve was charged with complex **4** (11 mg, 0.016 mmol), dissolved in 0.5 mL toluene-d₈ and pressurized with 2.5 bar CO₂. The exchange reaction was monitored by ¹H and ³¹P{¹H} NMR spectroscopy. After 20 h at ambient temperature complex **5** was formed in ca. 10% yield. Heating the tube for 24 h at 100°C gave complex **3** in 75% yield. Free H₂ gas was detected in the ¹H NMR spectrum as singlet at 4.46 ppm.

cis-[Re(PNP^{tBu})(CO)₂D] (4a): A *J. Young* NMR tube, fitted with a *Kontes* valve, was charged with complex **2** (25 mg, 0.039 mmol), dissolved in 0.6 mL toluene-d₈ and subsequently pressurized with 1 bar D₂ gas. The green solution turned instantly yellow and **4a** was obtained in quantitative yield. ¹H NMR (500.13 MHz, tol-d₈, 25°C) δ: 1.29 (m, 18H, (CH₃)₃CP), 1.38 (m, 18H, (CH₃)₃CP), 3.12 (dt, ²J_{HH} = 16.00 Hz, J = 2.50 Hz, 2H, PCH₂), 3.17 (m, 3H, PCH₂ + PCHD), 6.47 (d, ³J_{HH} = 7.50 Hz, 2H, CH_{py}), 6.80 (t, ³J_{HH} = 7.50 Hz, 1H, CH_{py(4)}), ppm. ³¹P{¹H} NMR (202.5 MHz, C₆D₆, 25°C) δ: 83.7 (m, 2P, ²J_{PD} = not resolved, for spectra see ESI) ppm. ¹³C{¹H} NMR (125.8 MHz, toluene-d₈, 25°C) δ: 29.8 (br, m, 12C, (CH₃)₃CP), 35.5 (dd, J = 7.5 Hz, 2C, (CH₃)₃CP), 37.6 (m, 2C, (CH₃)₃CP), 41.8 (br, m, 1C, PCHD), 42.1 (dd, ¹J_{CP} = 10.3 Hz, ³J_{PC} = 5.2 Hz, 1C, PCH₂), 118.8 (br, m, 2C, CH_{py}), 134.4 (s, 1C, CH_{py(4)}), 164.5 (m, 2C, C_{py}), 208.5 (t, ²J_{CP} = 5.3 Hz, 1C, Re-CO), 208.6 (t, ²J_{CP} = 5.0 Hz, 1C, Re-CO) ppm. **H/D exchange experiment:** The obtained solution of **4a** in toluene-d₈ (0.5 mL) as described above was degassed by two freeze-pump-thaw cycles and pressurized with H₂ gas (1 bar). The H/D exchange reaction was followed by ¹H NMR spectroscopy. Heating the sample for at 60 °C for 1 h gave complex **4b** in 70% yield,

increasing the reaction time to 48 h completed the transformation. Heating the solution of **4b** in a *J. Young* NMR tube at 130°C under H₂ pressure (2 bar) for 2 h gave complex **4** in 56% yield. Heating for 30 min at 160°C under a pressure of 2 bars of H₂ resulted in the formation of **4** (91% yield). (¹H NMR spectroscopic details are given in the ESI, Figure S18–S21)

cis-[Re(PNP^tBu)(CO)₂(OOCH)] (5): KO^tBu (10 mg, 0.09 mmol, 1 equiv.) was added to a stirred solution of **1** (60 mg, 0.09 mmol) in 3 mL THF in a 20 mL vial. After 10 min all volatiles were evaporated *in vacuo* and the residue was extracted with *n*-pentane (15 mL) and filtered through a syringe filter (Teflon, 0.2 μm pore size). Subsequently, formic acid (one drop via Pasteur pipette) was added and an immediate color change to yellow occurred. A slightly yellow precipitate was formed, which was decanted from the mother liquor and washed with *n*-pentane and dried *in vacuo* to give **5**. Yield: 47 mg, 82%. ¹H NMR (500.13 MHz, C₆D₆, sparsely soluble, 25°C) δ: 1.12 (vt, AA'BB', ³J_{PH} = 6.50 Hz, 18H, (CH₃)₃CP), 1.18 (vt, AA'BB', ³J_{PH} = 6.50 Hz, 18H, (CH₃)₃CP), 3.08 (dt, ²J_{HH} = 15.50 Hz, *J* = 3.50 Hz, 2H, PCH₂), 3.61 (dt, ²J_{HH} = 15.5 Hz, *J* = 3.50 Hz, 2H, PCH₂), 6.48 (d, ³J_{HH} = 7.50 Hz, 2H, CH_{py}), 6.84 (t, ³J_{HH} = 7.50 Hz, 1H, CH_{py(4)}), 8.94 (s, 1H, Re–OOCH) ppm. ³¹P{¹H} NMR (202.5 MHz, C₆D₆, sparsely soluble 25°C) δ: 72.3 (s, 2P) ppm. ¹³C{¹H} NMR (125.8 MHz, C₆D₆, sparsely soluble, 25°C) δ: 30.4 (vt, ²J_{CP} = 1.8 Hz, 6C, (CH₃)₃CP), 30.7 (vt, ²J_{CP} = 2.0 Hz, 6C, (CH₃)₃CP), 36.8 (t, ¹J_{CP} = 6.8 Hz, 2C, (CH₃)₃CP), 38.0 (t, ¹J_{CP} = 89.7 Hz, 2C, (CH₃)₃CP), 38.7 (t, ¹J_{CP} = 7.2 Hz, 2C, PCH₂), 120.4 (br, m, 2C, CH_{py}), 136.9 (s, 1C, CH_{py(4)}), 165.3 (t, *J*_{PC} = 3.6 Hz, 2C, C_{py}), 170.8 (br, s, 1C, Re–OOCH), 205.3 (br, m, 1C, Re–CO), 208.2 (br, m, 1C, Re–CO) ppm. IR (KBr, pellet) ν[cm⁻¹]: 1907, 1824 (ν_{CO}, 1:1 ratio), 1630 (ν_{COOH}). Elemental analysis: (C₂₆H₄₄N₁O₄P₂Re) calculated (found): C 45.74 (45.58) H 6.50 (6.45) N 2.05 (1.48) %. MS (ESI-TOF) calc. 683.23; found M⁺ = 638.36 (5⁺–COOH), 706.31 (5 + Na⁺).

CO₂ insertion in Re–H bond: A *J. Young* NMR tube, fitted with a *Kontes* valve, was charged with complex **4** (10 mg, 0.016 mmol), dissolved in 0.5 mL C₆D₆ and pressurized with 2 bars CO₂. The reaction was followed by ¹H and ³¹P{¹H} NMR spectroscopy. After 70 h at 50°C complex **5** was formed in 77% yield.

Acknowledgments

This research was supported by the European Research Council under the FP7 framework (ERC No 246837). DM is the Israel Matz Professorial Chair of Organic Chemistry. MV thanks the Swiss Friends of the Weizmann Institute of Science for a postdoctoral fellowship.

Notes and References

ELECTRONIC SUPPLEMENTARY INFORMATION (ESI) available (Figures giving NMR spectra, further experimental details). CORRESPONDING AUTHOR: * Prof. Dr. D. Milstein, E-mail: david.milstein@weizmann.ac.il

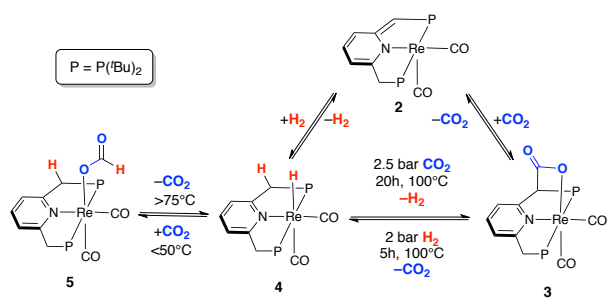
ABBREVIATIONS: Used abbreviations in reported NMR spectra: singlet (s), doublet (d), doublet of doublet (dd), doublet of doublets (ddd), triplet (t), virtual triplet (vt), multiplet (m).

Notes and References

1. T. Schaub and R. A. Paciello, *Angew. Chem. Int. Ed.*, 2011, **50**, 7278–7282.
2. M. He, Y. Sun, and B. Han, *Angew. Chem. Int. Ed.*, 2013, **52**, 9620–9633.
3. E. A. Quadrelli, G. Centi, J.-L. Duplan, and S. Perathoner, *ChemSusChem*, 2011, **4**, 1194–1215.
4. G. A. Olah, A. Goepfert, and G. K. S. Prakash, *Beyond Oil and Gas: the Methanol Economy*, 2006.
5. M. Cokoja, C. Bruckmeier, B. Rieger, W. A. Herrmann, and F. E. Kühn, *Angew. Chem. Int. Ed.*, 2011, **50**, 8510–8537.
6. I. Castro-Rodriguez, H. Nakai, L. N. Zakharov, A. L. Rheingold, and K. Meyer, *Science*, 2004, **305**, 1757–1759.
7. P. F. Souter and L. Andrews, *J. Am. Chem. Soc.*, 1997, **119**, 7350–7360.
8. H. Mauser, W. A. King, J. E. Greedy, and T. J. Andrews, *J. Am. Chem. Soc.*, 2001, **123**, 10821–10829.
9. H.-J. Lee, M. D. Lloyd, K. Harlos, I. J. Clifton, J. E. Baldwin, and C. J. Schofield, *J. Mol. Biol.*, 2001, **308**, 937–948.
10. V. T. Annibale and D. Song, *Chem. Commun. (Camb.)*, 2012, **48**, 5416–5418.
11. S. R. Flynn and D. F. Wass, *ACS Catal.*, 2013, **3**, 2574–2581.
12. A. M. Chapman, M. F. Haddow, and D. F. Wass, *J. Am. Chem. Soc.*, 2013, **133**, 18463–18478.
13. X. Xu, G. Kehr, C. G. Daniliuc, and G. Erker, *J. Am. Chem. Soc.*, 2013, **135**, 6465–6476.
14. D. A. Dickie, E. N. Coker, and R. A. Kemp, *Inorg. Chem.*, 2011, **50**, 11288–11290.
15. D. A. Dickie, R. P. Ulibarri-Sanchez III, P. J. Jarman, and R. A. Kemp, *Polyhedron*, 2013, **58**, 92–98.
16. M. J. Sgro and D. W. Stephan, *Angew. Chem. Int. Ed.*, 2012, **51**, 11343–11345.
17. M. J. Sgro and D. W. Stephan, *Chem. Commun.*, 2013, **49**, 2610–2612.
18. M.-A. Courtemanche, J. Larouche, M.-A. Légaré, W. Bi, L. Maron, and F.-G. Fontaine, *Organometallics*, 2013, **32**, 6804–6811.
19. P. Braunstein, D. Matt, Y. Dusausoy, J. Fischer, A. Mitschler, and L. Ricard, *J. Am. Chem. Soc.*, 1981, **103**, 5115–5125.
20. F. A. LeBlanc, A. Berkefeld, W. E. Piers, and M. Parvez, *Organometallics*, 2012, **31**, 810–818.
21. M. Vogt, M. Gargir, M. A. Iron, Y. Diskin-Posner, Y. Ben-David, and D. Milstein, *Chem.-Eur. J.*, 2012, **18**, 9194–9197.
22. C. A. Huff, J. W. Kampf, and M. S. Sanford, *Organometallics*, 2012, **31**, 4643–4645.
23. C. Gunanathan and D. Milstein, *Science*, 2013, **341**, 1229712.
24. C. Gunanathan and D. Milstein, *Top Organometal. Chem.*, 2011, **37**, 55–84.
25. C. Gunanathan and D. Milstein, *Acc. Chem. Res.*, 2011, **44**, 588–602.
26. R. Noyori, M. Koizumi, D. Ishii, and T. Ohkuma, 2001, vol. 73, pp. 227–232.
27. S. Clapham, A. Hadzovic, and R. Morris, *Coordin Chem Rev*, 2004, **248**, 2201–2237.
28. T. Ikariya and A. J. Blacker, *Acc. Chem. Res.*, 2007, **40**, 1300–1308.
29. H. Grützmacher, *Angew. Chem. Int. Ed.*, 2008, **47**, 1814–1818.

30. Y. Blum, D. Czarkie, Y. Rahamim, and Y. Shvo, *Organometallics*, 1985, **4**, 1459–1461.
31. T. Ikariya and M. Shibasaki, *Bifunctional Molecular Catalysis*, Springer, Berlin, Heidelberg, 1st edn. 2011, vol. 37.
32. A. Friedrich and S. Schneider, *ChemCatChem*, 2009, **1**, 72–73.
33. R. Tanaka, M. Yamashita, and K. Nozaki, *J. Am. Chem. Soc.*, 2011, **131**, 14168–14169.
34. R. Tanaka, M. Yamashita, L. W. Chung, K. Morokuma, and K. Nozaki, *Organometallics*, 2011, **30**, 6742–6750.
35. T. Koike and T. Ikariya, *Adv. Synth. & Cat.*, 2004, **346**, 37–41.
36. R. Langer, Y. Diskin-Posner, G. Leitus, L. J. W. Shimon, Y. Ben-David, and D. Milstein, *Angew. Chem. Int. Ed.*, 2011, **50**, 9948–9952.
37. G. A. Filonenko, M. P. Conley, C. Copéret, M. Lutz, E. J. M. Hensen, and E. A. Pidko, *ACS Catal.*, 2013, **3**, 2522–2526.
38. E. Balaraman, C. Gunanathan, J. Zhang, L. J. W. Shimon, and D. Milstein, *Nature Chem*, 2011, **3**, 609–614.
39. C. A. Huff and M. S. Sanford, *J. Am. Chem. Soc.*, 2012, **133**, 18122–18125.
40. Note that direct CO₂ hydrogenation to MeOH catalyzed by a tripodal Ru-phosphine catalyst was reported, see S. Wesselbaum, T. vom Stein, J. Klankermayer, and W. Leitner, *Angew. Chem. Int. Ed.*, 2012, **51**, 7499–7502.
41. M. Vogt, O. Rivada-Wheelaghan, M. A. Iron, G. Leitus, Y. Diskin-Posner, L. J. W. Shimon, Y. Ben-David, and D. Milstein, *Organometallics*, 2013, **32**, 300–308.
42. O. V. Ozerov, L. A. Watson, M. Pink, and K. G. Caulton, *J. Am. Chem. Soc.*, 2007, **129**, 6003–6016.
43. A. Choualeb, A. J. Lough, and D. G. Gusev, *Organometallics*, 2007, **26**, 3509–3515.
44. Y. Jiang, O. Blacque, T. Fox, and H. Berke, *J. Am. Chem. Soc.*, 2013, **135**, 7751–7760.
45. H.-F. Lang, P. E. Fanwick, and R. A. Walton, *Inorg Chim Acta*, 2002, **329**, 1–8.
46. S.-M. Kuang, P. E. Fanwick, and R. A. Walton, *Inorg. Chem.*, 2002, **41**, 405–412.
47. M. Vogt, A. Nerush, M. A. Iron, G. Leitus, Y. Diskin-Posner, L. J. W. Shimon, Y. Ben-David, and D. Milstein, *J. Am. Chem. Soc.*, 2013, **135**, 17004–17018.
48. L. Schwartzburd, M. A. Iron, L. Konstantinovski, E. Ben-Ari, and D. Milstein, *Organometallics*, 2011, **30**, 2721–2729.
49. L. Schwartzburd, M. A. Iron, L. Konstantinovski, Y. Diskin-Posner, G. Leitus, L. J. W. Shimon, and D. Milstein, *Organometallics*, 2010, **29**, 3817–3827.
50. E. Ben-Ari, G. Leitus, L. J. W. Shimon, and D. Milstein, *J. Am. Chem. Soc.*, 2006, **128**, 15390–15391.
51. J. Zhang, G. Leitus, Y. Ben-David, and D. Milstein, *J. Am. Chem. Soc.*, 2005, **127**, 10840–10841.
52. The incorporation of deuterium occurs in both pincer arms of **4a**. This can be a result of deprotonation of complex **1** occurring statistically on both *exo*-cyclic CH₂ groups of **1**, as well as a result of possible rapid conversion between two equivalent square pyramidal structures of the dearomatized complex **2** in solution.⁴⁷ Therefore a diastereomeric mixture is formed, which leads to complex patterns for the CH₂/CHD resonances in the ¹H NMR spectrum. However, the ¹H{³¹P} NMR spectrum (400 MHz, toluene-*d*₈) gave sufficient resolution and two doublet resonances were found at 3.20 ppm and 3.14 ppm, respectively, with a large geminal coupling constant of ²J_{HH} 16= Hz (Figure S23 in *ESI*). Integration of both resonances gave a ratio of 1:2, which indicates the selective incorporation of one deuterium atom in mutual *syn* position to the Re–H moiety. This is reflected in the ¹H ¹H NOESY NMR spectrum of the diastereomeric mixture of hydrido complex **4b**. The resonances of the Re–H and the CHD moiety have mutual cross peaks with only one P–C(CH₃)₃ resonance, which suggests that the resonances are located on the same face of the central molecular plane (for spectral details see Figure S22 in *ESI*).
53. Seven coordinated Re complexes with hydrido and dihydrogen ligands were reported. Deuteride/ hydride exchange in **4a** may occur via such species: D. G. Gusev, D. Nietlispach, I. L. Eremenko, and H. Berke, *Inorg. Chem.*, 1993, **32**, 3628–3636.
54. Complex **4b** in toluene-*d*₈ solution was heated at 100°C under H₂ gas (1 bar) to form **4** in 43% yield after 24h, and 52% yield after 48h (for spectral details see *ESI* Figure S24–S25)
55. A. Boddien, D. Mellmann, F. Gärtner, R. Jackstell, H. Junge, P. J. Dyson, G. Laurenczy, R. Ludwig, and M. Beller, *Science*, 2011, **333**, 1733–1736.
56. R. Puddephatt and G. A. Yap, *Chem. Commun.*, 1998, 2365–2366.
57. Y. Himeda, *Green Chem.*, 2009, **11**, 2018–2022.
58. S. Oldenhof, B. de Bruin, M. Lutz, M. A. Sieglar, F. W. Patureau, J. I. van der Vlugt, and J. N. H. Reek, *Chem.-Eur. J.*, 2013, **19**, 11507–11511.
59. T. Zell, B. Butschke, Y. Ben-David, and D. Milstein, *Chem.-Eur. J.*, 2013, **19**, 8068–8072.
60. Note, when the formate complex **5** (0.03mol%) and formic acid were heated under reflux in dioxane in an open system for 24h transformation of HCOOH to CO₂ and H₂ was observed in only 27% yield. Extension of the reaction time to 48h gave 44% yield. The lower yields possibly a result of the lower reaction temperature in the open system
61. In a control experiment, formic acid was heated in dioxane in a Fischer–Porter tube at 180 °C for 1 h. The formation of gaseous products was not detected.

Table of Contents:



Metal-ligand cooperation in a rhenium PNP pincer complex gives rise to the reversible activation of CO₂ and H₂ and the efficient catalytic decomposition of formic acid under base-free conditions.